MOX–Report No. 15/2007

Multiscale modeling and simulation of drug release from cardiovascular stents

Christian Vergara, Paolo Zunino

MOX, Dipartimento di Matematica "F. Brioschi"
Politecnico di Milano, Via Bonardi 29 - 20133 Milano (Italy)

mox@mate.polimi.it http://mox.polimi.it

Multiscale modeling and simulation of drug release from cardiovascular stents *

Christian Vergara and Paolo Zunino♯

♯ MOX– Modellistica e Calcolo Scientifico
Dipartimento di Matematica "F. Brioschi"
Politecnico di Milano
via Bonardi 9, 20133 Milano, Italy
<christian.vergara,paolo.zunino>@polimi.it

Abstract

In this study, we focus on a specific application, the modeling and simulation of drug release from cardiovascular drug eluting stents. In particular, we analyze the drug release dynamics from the stent coating, where the drug is initially stored, to the arterial wall surrounding the stent. The main challenge in addressing this problem consists in accounting for multiple space scales. We propose a new multiscale model for the drug release that significantly cuts down the computational cost. This model allows us to consider a realistic problem setting, which is applied for the numerical experiments.

1 Introduction

Drug eluting stents (DES) are apparently simple medical implanted devices used to restore blood flow perfusion into stenotic arteries. However, the design of such devices is a very complex task because their performance in widening the arterial lumen and preventing further restenosis is influenced by many factors such as the geometrical design of the stent, the mechanical properties of the materials and the chemical properties of the drug that is released, as discussed in [13, 17].

*This work has been supported by Fondazione Cariplo, Milan, Italy, under the project "Modellistica matematica di materiali microstrutturati per dispositivi a rilascio di farmaco", by the Italian Institute of Technology (Istituto Italiano di Tecnologie) with the project "NanoBiotechnology - Models and Methods for Local Drug Delivery from Nano/Micro Structured Materials" and by the Policlinico di Milano with the project "Sistemi di Bioingegneria virtuale: Realizzazione di un modello per la identificazione e correzione dei difetti nel Sistema Venoso".

In this framework, mathematical models and numerical simulation techniques play a relevant role in understanding what are the most appropriate choices for the optimal design of DES. Indeed, several mathematical models have been developed to address the fundamental questions of pharmacokinetics, i.e. to estimate the total amount of drug to be released and the characteristic time scale of the release process. The model proposed by Higuchi, see [10, 11] is a milestone in this field. However, the drug release rate has been studied by Higuchi in one space dimension and for the case of constant coefficients, exploiting the analytical solutions of the governing equations in this simplified setting. For this reason, the Higuchi model and its variants are not suitable to address directly problems with complex geometries, such as the case of stents. Nevertheless, some of their restrictive assumptions have been removed in subsequent studies, we refer to [18] for an overview and in particular to [4] for the analysis of the case with time dependent coefficients. Recently, see [5], a more advanced model has been proposed for the study of the drug dose, namely the cumulative concentration along the release period, on an axialsymmetric geometrical setting. The work presented in [5] definitely overrides the main limitations of the original Higuchi model, but the fully three-dimensional and time dependent problem is not considered yet. This is the aim of the present work, that we address by means of a multiscale approach putting together the main ideas at the basis of the Higuchi model together with a general treatment of the geometrical setting. The resulting problem is then efficiently addressed by means of suitable numerical approximation techniques.

The main difficulties of this work arise from the need to deal with phenomena that take place on multiple scales in space and time. Concerning the space scales, we remind that DES for cardiovascular applications are miniaturized metal structures that are coated with a micro-film containing the drug that will be locally released into the arterial walls for healing purposes. The thickness of this film generally lays within the range of microns. As regards the time scales, we observe that the release of drug is deliberately very slow. In general, it persists until a few weeks after the stent implantation.

To address these topics, we start from a general model for mass transfer through heterogeneous media, consisting on an advection-diffusion-reaction equation for each different layer of material or tissue into the stent and the arterial walls, see for instance [15, 22]. Such model has already been applied in [12] for computational studies about drug release from stents. However, we point out that simulation studies based on this model involve extremely high computational costs and by consequence, to our knowledge, only studies concerning simplified stent geometries have been pursued so far. Starting from this point, we propose a multiscale model for mass transfer from a thin layer, which significantly cuts down the computational efforts needed for the simulation of the drug release from stents. Another difficulty arise from the fact that the simulation of drug release represents a stiff problem, whose

numerical approximation requires the application of an adaptive stepping strategy. For a preliminary analysis, we adopt the simple strategy proposed in [14] and we combine it with some a-priori knowledge of the behavior of the solution.

To sum up, combining a multiscale model for mass transfer with suitable numerical discretization methods it is possible to obtain simulations involving realistic expanded stent geometries, obtained in [19], and long time scales. The efficacy of our approach is demonstrated by means of numerical results concerning this realistic situation.

2 The mathematical model

2.1 General settings

Our mathematical model describing drug release from DES is basically obtained putting together a suitable model for the dynamics of the drug into the polymeric substrate with a corresponding model for mass transfer into the arterial walls. To this purpose, we assume that the tissues constituting the arteries as well as the stent coating behave as homogeneous and isotropic porous media with respect to the filtration of plasma and the transfer of molecules. In order to set up a mathematical model, we address at first the governing equations for the space dependence of the drug concentration in the stent coating and in the arterial walls. Then, the complete model is obtained by putting together these operators in the time dependent setting and balancing them with suitable forcing terms.

Concerning the dynamics of the drug inside the stent coating, we assume that it is simply governed by diffusion. As shown in [4], this assumption holds true when the initial concentration of the drug into the polymeric matrix is equal or very close to the solubility of the drug. In this case it is possible to neglect the phase transition process of the drug from the solid state to the dissolved state inside the matrix, and consider that all the drug is in the dissolved state from the beginning of the analysis. Exploiting a thermal analogy, we address a Stefan problem in the limit of high Stefan numbers.

We introduce a domain $\Omega_c \subset \mathbb{R}^3$ given by the thin polymeric layer surrounding the stent and we denote with $\boldsymbol{n}_c$ its outer unit normal vector. Moreover, let Γ be the interface between Ω_c and the arterial walls. Let $d(t, \boldsymbol{x})$ be the concentration of the dissolved drug in the coating, where t and $\boldsymbol{x}$ are the time and space coordinates respectively. We assume that $d(t, \boldsymbol{x})$ is governed by the diffusion operator $-D_c \Delta d$, where D_c is the diffusivity of the drug inside the polymer. This operator must be complemented by suitable boundary conditions that are determined observing that no drug transfer takes place from the stent coating to the metallic struts of the stent. Then, the space dependence of the concentration d is governed by the linear

operators $\mathfrak{L}_c d$ and $\mathfrak{B}_c d$ such that,

$$\mathfrak{L}_c d := -D_c \Delta d, \quad \text{in } \Omega_c,$$
$$\mathfrak{B}_c d := \nabla d \cdot \boldsymbol{n}_c, \quad \text{on } \partial\Omega_c \setminus \Gamma.$$

As regards the arteries, we remind that the arterial wall is a complex structure that consists in several concentric layers. Precisely, going from the lumen to the outer wall we find the endothelium, the intima, the internal elastic lamina, the media and finally the adventitia. Each layer has different physical properties. The plasma filtration and the transfer of molecules in such structure can be described by the so called *multilayer* model, introduced in [6] and evolved by [15] and [22] with the aim to analyze the absorption of low density lipoproteins into the arterial walls. However, we make here a simplification of the complex multilayered structure of the wall, more precisely we assume that the arterial wall is an homogeneous medium, whose physical properties are, for simplicity, the ones corresponding to the intermediate layer, namely the *media*. Furthermore, we neglect the dynamics of the drug into the blood flow. More precisely, we take into account that the drug released into the arterial wall may be partially transferred into the blood flow. This transfer takes place through a membrane of permeability P_w that represents the *endothelium*. However, once the drug has reached the blood flow, we assume that it is immediately transported away without influencing the downstream region of the artery.

In this context, let us consider the computational domain Ω_w, given by a truncated portion of the arterial wall, where Γ_a is the outer wall tissue, Γ_i is the interface with the blood, Γ_w are the artificial sections and Γ is the interface with the coating. We denote with $\boldsymbol{n}_w$ and $\boldsymbol{n}$ the unit normal vectors associated to Ω_w and $\Gamma = \partial\Omega_w \cap \partial\Omega_c$, respectively. The arbitrariness of the choice of $\boldsymbol{n}$ will not influence the set up of the model. A simplified shape of these domains is illustrated in Figure 1.

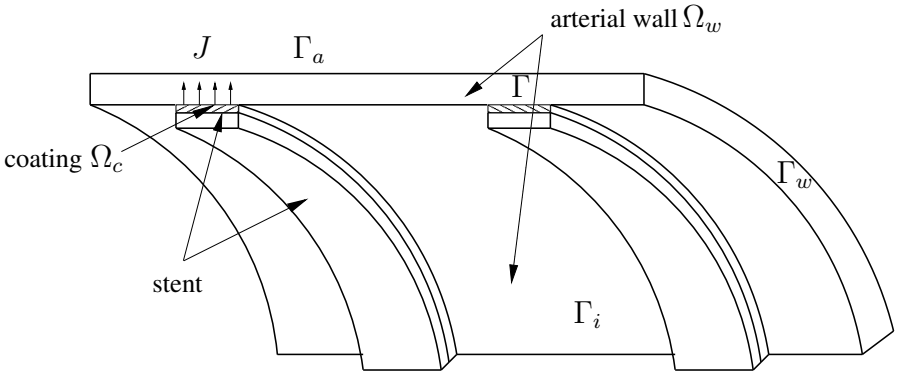

Figure 1: Computational domains Ω_w and Ω_c.

Let us denote with $a(t, \boldsymbol{x})$ the volume averaged concentration of the

drug dissolved into the plasma permeating the arterial walls. According to our physical assumptions, the dynamics of the concentration into the arterial walls is governed by the advection-diffusion operator $-D_w\Delta a + \boldsymbol{u}\cdot\nabla a$, where D_w is the diffusivity of the drug into the arterial tissue and $\boldsymbol{u}$ is the velocity field describing the filtration of the plasma inside the tissue. This operator is complemented by the following boundary conditions on $\partial\Omega_w$. At the interface Γ_i between the wall and the lumen we prescribe a homogeneous Robin condition $-D_w\nabla a\cdot\boldsymbol{n}_w - P_w a = 0$. Moreover, on the artificial boundaries, Γ_w, we prescribe a homogeneous Neumann condition $\nabla a\cdot\boldsymbol{n}_w = 0$, exploiting the circumferential and longitudinal periodicity of the stent struts. Then, we assume that the concentration is constant along the normal direction of the external wall Γ_a and then also on this part of boundary we prescribe $\nabla a\cdot\boldsymbol{n}_w = 0$. To summarize the governing equations for the concentration in the arterial walls, we introduce the linear operators $\mathfrak{L}_w a$ and $\mathfrak{B}_w a$ such that,

$$\mathfrak{L}_w a := -D_w\Delta a + \boldsymbol{u}\cdot\nabla a, \quad \text{in } \Omega_w,$$
$$\mathfrak{B}_w a := \begin{cases} -D_w\nabla a\cdot\boldsymbol{n}_w - P_w a & \text{on } \Gamma_i, \\ \nabla a\cdot\boldsymbol{n}_w & \text{on } \Gamma_a\cup\Gamma_w. \end{cases}$$

Finally, suitable *transmission conditions* must be satisfied by a and d at the interface Γ between Ω_w and Ω_c. Such conditions require the continuity of the concentration and of the corresponding flux according to Fick's law. They are summarized by the following operator,

$$\mathfrak{B}(a,d) := \begin{cases} a - d, & \text{on } \Gamma, \\ D_w\nabla a\cdot\boldsymbol{n} - D_c\nabla d\cdot\boldsymbol{n}, & \text{on } \Gamma. \end{cases}$$

Remark 2.1 In some cases, the polymeric coating on the stent is further covered by a thin film, which do not contains any drug, with the aim to slow down the release process. This additional layer is called *topcoat*. It is possible to model the topcoat as a membrane of infinitesimal thickness. In this case, the continuity of concentrations across Ω_c and Ω_w does not hold any more. By consequence, the first equation of $\mathfrak{B}(a,d)$ should be replaced by $-D_c\nabla d\cdot\boldsymbol{n}_c = P_\Gamma(d-a)$, where P_Γ is the permeability relative to the topcoat.

To proceed, according to [17, 26], we observe that the drug into the arterial wall can assume two different states: the state where the drug is dissolved into the plasma permeating the interstices between cells, whose volume averaged concentration is $a(t,\boldsymbol{x})$, and the state where the drug attaches to specific sites of the extra-cellular matrix of the tissue. Let us denote with $b(t,\boldsymbol{x})$ the density of the free binding sites in the tissue, with $b_0(\boldsymbol{x})$ their initial concentration in the arterial wall and with $c(t,\boldsymbol{x})$ the concentration of the drug attached to the extra-cellular matrix. We assume

that the drug in the state $c(t, \boldsymbol{x})$ can no longer diffuse or be transported by plasma. By virtue of the mass conservation principle, we immediately get $c(t, \boldsymbol{x}) = b_0(\boldsymbol{x}) - b(t, \boldsymbol{x})$. The equilibrium between the dissolved drug and the free binding sites is represented by the following equation,

$$a + b \overset{k_1}{\rightarrow} c, \quad c \overset{k_2}{\rightarrow} a + b, \quad \text{in } \Omega_w, \tag{1}$$

where k_1, k_2 are the association and dissociation constants. Then, the dynamics of the concentration in the arterial walls is also influenced by a reaction term,

$$\mathfrak{N}_w(a, b) := k_1 ab + k_2(b - b_0), \quad \text{in } \Omega_w.$$

We observe that $\mathfrak{N}_w(a, b)$ is a nonlinear operator that does not involve derivatives of a and b. Consequently it does not influence the boundary conditions represented by $\mathfrak{B}_w$.

To sum up, our pharmacokinetic model corresponds to the following system of equations that accounts for diffusion, transport and chemical binding of the drug inside the tissue, as well as diffusion inside the coating of the stent,

$$\begin{cases} \partial_t a + \mathfrak{L}_w a + \mathfrak{N}_w(a, b) = 0, & \text{in } (0, T] \times \Omega_w, \\ \partial_t d + \mathfrak{L}_c d = 0, & \text{in } (0, T] \times \Omega_c, \\ \partial_t b + \mathfrak{N}_w(a, b) = 0, & \text{in } (0, T] \times \Omega_w, \\ \mathfrak{B}_w a = 0, & \text{on } (0, T] \times \partial\Omega_w \setminus \Gamma, \\ \mathfrak{B}_c d = 0, & \text{on } (0, T] \times \partial\Omega_c \setminus \Gamma, \\ \mathfrak{B}(a, d) = 0, & \text{on } (0, T] \times \Gamma, \end{cases} \tag{2}$$

together with suitable initial conditions that prescribe that the drug is initially gathered only into the stent coating with uniform concentration $d_0 > 0$, namely we set:

$$a|_{t=0} = a_0 = 0, \quad b|_{t=0} = b_0, \quad d|_{t=0} = d_0.$$

Finally, the velocity field $\boldsymbol{u}(t, \boldsymbol{x})$ describing the plasma filtration through the arterial walls together with the corresponding pressure $p(t, \boldsymbol{x})$ are governed by means of the Darcy's law of filtration,

$$\boldsymbol{u} = -\frac{k_b}{\mu_b} \nabla p, \quad \nabla \cdot \boldsymbol{u} = 0, \quad \text{in } \Omega_w,$$

where k_b and μ_b are the hydraulic permeability of the arterial walls and the viscosity of the blood plasma respectively. To prescribe suitable boundary conditions we require that $\boldsymbol{u} \cdot \boldsymbol{n}_w = 0$ on Γ_w for symmetry and that $\boldsymbol{u} \cdot \boldsymbol{n}_w = 0$ on Γ because we assume that the plasma can not penetrate inside the stent coating. Moreover, we observe that the filtration of plasma inside the arterial

walls is driven by a decreasing pressure gradient from the inner to the outer part of the artery. By consequence, setting the zero level of the pressure to the standard atmospheric pressure, we require that $p = \delta p(t)$ on Γ_i and $p = 0$ on Γ_a, where $70 \leq \delta p(t) \leq 120$ mmHg is the over-pressure induced by the heartbeat. We notice that $\delta p(t)$ is assumed to be uniform, and thus independent of $\boldsymbol{x} \in \Gamma_i$. In conclusion, the filtration velocity inside the arterial walls is governed by the operator,

$$\mathfrak{D}(\boldsymbol{u}, p) := \begin{cases} \boldsymbol{u} + \frac{k_b}{\mu_b} \nabla p & \text{in } \Omega_w, \\ \nabla \cdot \boldsymbol{u} & \text{in } \Omega_w, \\ p & \text{on } \Gamma_a, \\ p - 1 & \text{on } \Gamma_i, \\ \nabla p \cdot \boldsymbol{n}_w & \text{on } \Gamma_w \cup \Gamma, \end{cases}$$

and exploiting the linearity of the previous operator the desired velocity and pressure are given by the following problem,

$$\begin{array}{ll} \mathfrak{D}(\bar{\boldsymbol{u}}, \bar{p}) = 0, & \text{in } \Omega_w, \quad \mathfrak{D}(\bar{\boldsymbol{u}}, \bar{p}) = 0 \quad \text{on } \partial\Omega_w, \\ \boldsymbol{u}(t, \boldsymbol{x}) = \delta p(t) \cdot \bar{\boldsymbol{u}}(\boldsymbol{x}), & p(t, \boldsymbol{x}) = \delta p(t) \cdot \bar{p}(\boldsymbol{x}). \end{array} \tag{3}$$

Equation (2) represents to our knowledge the most realistic model to describe the drug release from the stent. It consists of two second-order parabolic partial differential equations on adjacent domains, $(2)_a$ and $(2)_b$, respectively, coupled by means of the transmission conditions on Γ expressed by $(2)_f$. Moreover, to take into account the reactions between the drug and the arterial tissue, we also consider the zero-order partial differential equation $(2)_c$, in other words an ordinary differential equation for each point of Ω_w. This equation couples a and b nonlinearly. It is clear that the numerical approximation of equation (2) is a very challenging task. The aim of this work is to develop suitable strategies and algorithms that make it possible to apply (2) to a realistic problem.

2.2 Outline of the analysis of the coupled problem

In this section we look at the main lines of the well posedness analysis of the model. Since this is not the principal objective of this work, we will not address rigorously all the details of this study.

Problem (2) features two different kind of difficulties. On one side, the unknowns $a(t, \boldsymbol{x})$ and $b(t, \boldsymbol{x})$ are coupled on Ω_w by means of the nonlinear term $\mathfrak{N}_w(a, b)$. On the other side, $a(t, \boldsymbol{x})$ and $d(t, \boldsymbol{x})$ interact on Γ through linear transmission conditions.

In order to simplify the technicalities of this analysis, even though this does not correspond to the geometrical configuration of our reference application, we assume that $\Omega_c,\ \Omega_w \subset \mathbb{R}^3$ are open and connected domains

with regular boundaries $\partial\Omega_c,\ \partial\Omega_w$ of class $C^{1+\epsilon}$ with $\epsilon > 0$. This is easily verified if Ω_c is embedded into Ω_w. Furthermore, we remind that the operators $\mathfrak{L}_c$ and $\mathfrak{L}_w$ are characterized by constant coefficients and we assume that the corresponding initial and boundary conditions are compatible. We immediately observe that the initial conditions for a and d are incompatible with the interface equation $\mathfrak{B}(a,d) = 0$ on Γ. To override this drawback we restrict our analysis to $(0,T]$. By consequence, given a generic domain for the space variables Ω, we look for solutions in the following space,

$$\begin{aligned}\mathcal{S}(\Omega,T) := \{&u(t,\boldsymbol{x}) \in C^0\big((0,T]\times\bar{\Omega}\big) \text{ s.t.}\\ &u(\cdot,\boldsymbol{x}) \in C^1\big((0,T]\big)\ \forall \boldsymbol{x}\in\Omega \text{ and } u(t,\cdot)\in C^2(\Omega)\ \forall t\in(0,T]\}.\end{aligned}$$

In what follows, we will consider the triplets of functions $(a,b,d) \in \mathcal{S}(\Omega_w,T)\times\mathcal{S}(\Omega_w,T)\times\mathcal{S}(\Omega_c,T)$. For simplicity, we introduce $\mathbf{S} := \mathcal{S}(\Omega_w,T)\times\mathcal{S}(\Omega_w,T)\times\mathcal{S}(\Omega_c,T)$.

Then, in order to prove the existence of such problem, we follow the framework proposed by Pao, see [20], Chapter 8. First of all, let us introduce the definition of upper and lower solutions of problem (2). In particular, the triplets $(\tilde{a},\tilde{b},\tilde{d}),\ (\hat{a},\hat{b},\hat{d}) \in \mathbf{S}$ are called upper and lower solutions of (2) if they satisfy respectively,

$$\begin{cases}
\partial_t\tilde{a} + \mathfrak{L}_w\tilde{a} + \mathfrak{N}_w(\tilde{a},\tilde{b}) \geq 0, & \partial_t\hat{a} + \mathfrak{L}_w\hat{a} + \mathfrak{N}_w(\hat{a},\hat{b}) \leq 0 & \text{in } (0,T]\times\Omega_w,\\
\partial_t\tilde{d} + \mathfrak{L}_c\tilde{d} \geq 0, & \partial_t\hat{d} + \mathfrak{L}_c\hat{d} \leq 0, & \text{in } (0,T]\times\Omega_c,\\
\partial_t\tilde{b} + \mathfrak{N}_w(\tilde{a},\tilde{b}) \geq 0, & \partial_t\hat{b} + \mathfrak{N}_w(\hat{a},\hat{b}) \leq 0, & \text{in } (0,T]\times\Omega_w,\\
\mathfrak{B}_w\tilde{a} \geq 0, & \mathfrak{B}_w\hat{a} \leq 0, & \text{on } (0,T]\times\partial\Omega_w\setminus\Gamma,\\
\mathfrak{B}_c\tilde{d} \geq 0, & \mathfrak{B}_c\hat{d} \leq 0, & \text{on } (0,T]\times\partial\Omega_c\setminus\Gamma,\\
\mathfrak{B}(\tilde{a},\tilde{d}) = 0, & \mathfrak{B}(\hat{a},\hat{d}) = 0, & \text{on } (0,T]\times\Gamma,\\
\tilde{a} - a_0 \geq 0, & \hat{a} - a_0 \leq 0, & \text{on } \{t=0\}\times\Omega_w,\\
\tilde{d} - d_0 \geq 0, & \hat{d} - d_0 \leq 0, & \text{on } \{t=0\}\times\Omega_c,\\
\tilde{b} - b_0, \geq 0, & \hat{b} - b_0, \leq 0, & \text{on } \{t=0\}\times\Omega_w.
\end{cases}$$

We notice that in these definitions we require that the interface conditions between Ω_w and Ω_c, coupling a and d, are exactly satisfied. This prevents the arbitrary choice of the signs in the operator $\mathfrak{B}(a,d)$ to influence the analysis of the problem.

Property 1 *The triplets* $(\tilde{a},\tilde{b},\tilde{d}) = (d_0,b_0,d_0)$ *and* $(\hat{a},\hat{b},\hat{d}) = (0,0,0)$ *are upper and lower solutions of problem* (2).

According to this result, we define $\mathbf{B}$ as the sector of $\mathbf{S}$ such that,

$$\mathbf{B} := \{(a,b,d) \in \mathbf{S} \text{ s.t. } 0 \leq a(t,\boldsymbol{x}) \leq d_0,\ 0 \leq b(t,\boldsymbol{x}) \leq b_0,\ 0 \leq d(t,\boldsymbol{x}) \leq d_0\}.$$

Property 2 *The function* $\mathfrak{N}_w(a,b)$ *is Lipschitz continuous and monotone non-decreasing in* $[\hat{a},\tilde{a}]\times[\hat{b},\tilde{b}] = [0,d_0]\times[0,b_0]$.

Then, we propose a constructive method to identify a solution of the problem at hand. Given suitable initial guesses $(\tilde{a}, \hat{b}, \hat{d})$, $(\hat{a}, \tilde{b}, \tilde{d})$, by means of the following linear problems we build up two corresponding sequences, that we denote with $(\overline{a}^{(k)}, \underline{b}^{(k)}, \underline{d}^{(k)})$, $(\underline{a}^{(k)}, \overline{b}^{(k)}, \overline{d}^{(k)}) \in \mathbf{S}$ respectively,

$$\begin{cases} \partial_t a^{(k)} + \mathfrak{L}_w a^{(k)} = \mathfrak{F}_w(a^{(k-1)}, b^{(k-1)}), & \text{in } (0,T] \times \Omega_w, \\ \partial_t d^{(k)} + \mathfrak{L}_c d^{(k)} = 0, & \text{in } (0,T] \times \Omega_c, \\ \mathfrak{B}_w a^{(k)} = 0, & \text{on } (0,T] \times \partial\Omega_w \setminus \Gamma, \\ \mathfrak{B}_c d^{(k)} = 0, & \text{on } (0,T] \times \partial\Omega_c \setminus \Gamma, \\ \mathfrak{B}(a^{(k)}, d^{(k)}) = 0, & \text{on } (0,T] \times \Gamma, \\ a^{(k)} = a_0, & \text{on } \{t=0\} \times \Omega_w, \\ d^{(k)} = d_0, & \text{on } \{t=0\} \times \Omega_c, \end{cases} \tag{4}$$

$$\begin{cases} \partial_t b^{(k)} = \mathfrak{F}_w(a^{(k-1)}, b^{(k-1)}), & \text{in } (0,T] \times \Omega_w, \\ b^{(k)} = b_0, & \text{on } \{t=0\} \times \Omega_w, \end{cases} \tag{5}$$

where $\mathfrak{F}_w(a,b) := -\mathfrak{N}_w(a,b)$. The existence and uniqueness of weak solutions $a^{(k)} \in L^2\big(0,T; H^1(\Omega_w)\big)$ and $d^{(k)} \in L^2\big(0,T; H^1(\Omega_c)\big)$ is ensured by the fundamental principles of domain decomposition methods, see [24] for a general treatment and [25] for the specific case of problem (4). Moreover, thanks to the regularity of the domain and of the data, we also conclude that the weak solution coincides with the strong one, precisely $a^{(k)} \in \mathcal{S}(\Omega_w, T)$ and $d^{(k)} \in \mathcal{S}(\Omega_c, T)$. As regards problem (5), we notice that it can be seen as an initial value problem depending on the parameter $\boldsymbol{x} \in \Omega_w$. By virtue of the Picard-Lindelof theorem, see [9], and thanks to the regularity of $a(t, \boldsymbol{x})$ and $\mathfrak{F}_w(a,b)$, we conclude that it admits a solution in $\mathcal{S}(\Omega_w, T)$ for any $T > 0$. Furthermore, we will make use of the following multi-domain version of a classical positivity property of linear parabolic operators, see for instance [20], Lemma 2.2.1.

Lemma 1 *Let $a \in \mathcal{S}(\Omega_w, T)$ and $d \in \mathcal{S}(\Omega_c, T)$ be such that,*

$$\begin{cases} \partial_t a + \mathfrak{L}_w a \geq 0, & \textit{in } (0,T] \times \Omega_w, \\ \partial_t d + \mathfrak{L}_c d \geq 0, & \textit{in } (0,T] \times \Omega_c, \\ \mathfrak{B}_w a \geq 0, & \textit{on } (0,T] \times \partial\Omega_w \setminus \Gamma, \\ \mathfrak{B}_c d \geq 0, & \textit{on } (0,T] \times \partial\Omega_c \setminus \Gamma, \\ \mathfrak{B}(a,d) = 0, & \textit{on } (0,T] \times \Gamma, \\ a \geq 0, & \textit{on } \{t=0\} \times \Omega_w, \\ d \geq 0, & \textit{on } \{t=0\} \times \Omega_c. \end{cases}$$

Then, $a \geq 0$ in $[0,T] \times \Omega_w$ and $d \geq 0$ in $[0,T] \times \Omega_c$.

Sketch of the proof. This property holds true because problem (4) is equivalent, in the sense of weak solutions, to a single-domain problem featuring discontinuous coefficients on Ω. Then, we recover Lemma 1 exploiting

the single-domain positivity result applied to weak solutions, which is obtained by means of a cut-off technique (see for instance [7]) together with the additional regularity results arising from the smoothness of the sub-domains and of the local data. □

To proceed, mimicking Lemma 8.2.2 of [20], we assert that the sequences $(\overline{a}^{(k)}, \underline{b}^{(k)}, \underline{d}^{(k)})$ and $(\underline{a}^{(k)}, \overline{b}^{(k)}, \overline{d}^{(k)})$ satisfy the following property.

Lemma 2 *If Propositions 1 and 2 hold true, then the sequences* $(\overline{a}^{(k)}, \underline{b}^{(k)}, \underline{d}^{(k)})$ *and* $(\underline{a}^{(k)}, \overline{b}^{(k)}, \overline{d}^{(k)})$ *satisfy the following inequalities*

$$\underline{w}^{(k-1)} \leq \underline{w}^{(k)} \leq \overline{w}^{(k)} \leq \overline{w}^{(k-1)} \text{ for } w = a, b, d. \tag{6}$$

Sketch of the proof. The proof can be subdivided in three steps.
First step: we set $\underline{a}^{(0)} = \hat{a}$, $\overline{b}^{(0)} = \tilde{b}$, $\overline{d}^{(0)} = \tilde{d}$ and we introduce the following auxiliary functions,

$$\underline{r}^{(0)} = \underline{a}^{(1)} - \underline{a}^{(0)}, \quad \overline{s}^{(0)} = \overline{b}^{(0)} - \overline{b}^{(1)}, \quad \overline{z}^{(0)} = \overline{d}^{(0)} - \overline{d}^{(1)}.$$

We replace them into problems (4), (5) and we apply Lemma 1 together with the trivial conclusion that $\partial_t \overline{s}^{(0)} \geq 0$ and $\overline{s}^{(0)}(t=0) \geq 0$ imply $\overline{s}^{(0)} \geq 0$ for $t > 0$. By this way, we assert that $\underline{r}^{(0)} \geq 0$, $\overline{s}^{(0)} \geq 0$, $\overline{z}^{(0)} \geq 0$, or equivalently

$$\underline{a}^{(1)} \geq \underline{a}^{(0)}, \quad \overline{b}^{(1)} \leq \overline{b}^{(0)}, \quad \overline{d}^{(1)} \leq \overline{d}^{(0)}.$$

Second step: we set $\overline{a}^{(0)} = \tilde{a}$, $\underline{b}^{(0)} = \hat{b}$, $\underline{d}^{(0)} = \hat{d}$ and correspondingly,

$$\overline{r}^{(0)} = \overline{a}^{(0)} - \overline{a}^{(1)}, \quad \underline{s}^{(0)} = \underline{b}^{(1)} - \underline{b}^{(0)}, \quad \underline{z}^{(0)} = \underline{d}^{(1)} - \underline{d}^{(0)}.$$

Proceeding as in the first step we obtain, $\overline{a}^{(1)} \leq \overline{a}^{(0)}$, $\underline{b}^{(1)} \geq \underline{b}^{(0)}$, $\underline{d}^{(1)} \geq \underline{d}^{(0)}$.
Third step: we introduce $r^{(1)} = \overline{a}^{(1)} - \underline{a}^{(1)}$, $s^{(1)} = \overline{b}^{(1)} - \underline{b}^{(1)}$, $z^{(1)} = \overline{d}^{(1)} - \underline{d}^{(1)}$ and exploiting again the positivity lemma we assert that $r^{(1)}$, $s^{(1)}$, $z^{(1)} \geq 0$. This allows us to conclude that,

$$\underline{w}^{(0)} \leq \underline{w}^{(1)} \leq \overline{w}^{(1)} \leq \overline{w}^{(0)}, \text{ with } w = a, b, d.$$

The result (6) follows by means of the recursive application of the three steps. □

Finally, we conclude this analysis with the following result that is obtained mimicking Theorem 8.3.2 of [20], to which we refer for a detailed proof.

Theorem 2.2 (Existence and uniqueness) *Under assumptions of Lemma 2, problem* (2) *admits a unique solution* $(a, b, d) \in \mathbf{B}$. *Moreover, the sequences* $(\overline{a}^{(k)}, \underline{b}^{(k)}, \underline{d}^{(k)})$, $(\underline{a}^{(k)}, \overline{b}^{(k)}, \overline{d}^{(k)})$ *converge to* (a, b, d) *as referred by* (6).

Sketch of the proof (existence). The existence of solutions is obtained combining Lemma 2, the dominated convergence theorem and the integral representation by means of Green's functions of the solutions of the linear problems (4) and (5). □

Theorem 2.2 is also interesting from a more applicative perspective, because it suggests that the solution of the coupled problem (2) can be approximated by means of a fixed point iterative procedure. Moreover, it has the following straightforward consequences that will be particularly useful in the development of a multiscale model.

Property 3 (Boundedness) *Owing to Theorem 2.2 and to the definition of* $\mathbf{B}$*, the solution of problem* (2) *satisfy,*

$$
\begin{aligned}
&0 \leq a(t,\boldsymbol{x}) \leq d_0,\ \forall (t,\boldsymbol{x}) \in [0,T] \times \Omega_w,\\
&0 \leq b(t,\boldsymbol{x}) \leq b_0,\ \forall (t,\boldsymbol{x}) \in [0,T] \times \Omega_w,\\
&0 \leq d(t,\boldsymbol{x}) \leq d_0,\ \forall (t,\boldsymbol{x}) \in [0,T] \times \Omega_c.
\end{aligned}
$$

Property 4 (Maximum Principle) *Owing to Proposition 3 and to the Maximum Principle (see for instance Theorem 2.1.5, [20]), the maximum of* $a(t,\boldsymbol{x})$ *lies on* $\partial\Omega_w$ *for any* $t > 0$*. Furthermore, because* Γ *is the only subset of* $\partial\Omega_w$ *where* $\nabla a \cdot \boldsymbol{n}_w > 0$ *is admissible, the maximum of* $a(t,\boldsymbol{x})$ *lies on* Γ*.*

A direct consequence of Propositions 3 and 4 is that $a(t,\boldsymbol{x})$ is an increasing function with respect to time on any $\boldsymbol{x} \in \Gamma$, for suitably small times $t > 0$.

3 Reduced models for mass transfer from a thin layer

For the numerical discretization of problem (2) we aim to apply a finite difference scheme in time and a finite element method for the space dependence. For the second task, we need to build up a suitable computational mesh approximating Ω_w and Ω_c. In order to apply standard finite element solvers, it is useful that the computational meshes of Ω_w and Ω_c are conforming. Since Ω_c corresponds to a very thin layer, the construction of a reasonably regular computational mesh requires to consider many elements into Ω_c and also into the region of Ω_w neighboring Γ. From the computational viewpoint, this is a strong limitation to the efficacy of the finite element method for the simulation of our problem in realistic cases where Ω_c may be 7 μm thin, while Ω_w is comparable to a cylinder 2 mm wide and 10 mm long with a wall thickness of 0.5 mm, as illustrated in Figure 1. For this reason, in the next section we focus on the development of a multiscale model that allows us to approximate the mass transfer from a thin layer without the requirement to fully discretize the smaller scales. This overrides the problem to build up a computational mesh inside the thin coating.

First of all, let us describe the interface Γ by means of the mapping

$$\boldsymbol{x} : \omega \subset \mathbb{R}^2 \to \Gamma \subset \mathbb{R}^3, \quad \boldsymbol{x} = \boldsymbol{x}(\xi_1, \xi_2), \ \forall (\xi_1, \xi_2) \in \omega.$$

This mapping introduces a local system of curvilinear coordinates, whose covariant vectors are $\boldsymbol{a}_i = \partial_{\xi_i} \boldsymbol{x}$, $i = 1, 2$, $a_3 = (\boldsymbol{a}_1 \times \boldsymbol{a}_2)|\boldsymbol{a}_1 \times \boldsymbol{a}_2|^{-1}$. The vectors $\boldsymbol{a}_1$ and $\boldsymbol{a}_2$ define the tangent plane to Γ in the point $\boldsymbol{x}(\xi_1, \xi_2)$ and $\boldsymbol{a}_3$ is the normal unit vector to this plane. For each point $\boldsymbol{x} \in \Gamma$ we consider the tangent surface $d\sigma = (\boldsymbol{x} - \sum_{i=1}^{2} dx^i \boldsymbol{a}_i, \boldsymbol{x} + \sum_{i=1}^{2} dx^i \boldsymbol{a}_i)$ and the volume $dV = d\sigma \times [0, \Delta l]$, being Δl the thickness of the coating, assumed to be independent of $\boldsymbol{x} \in \Gamma$.

To set up a multiscale model, we remind that the coating is extremely thin and thus the concentration derivatives in the normal direction with respect to the coating surface are much higher with respect to the derivatives in the direction tangential to the surface. In other words, we assume that the drug concentration on the interface Γ, namely $a(t, \boldsymbol{x})$, is *quasi-uniform* with respect to the characteristic scale of the coating, which is Δl. As a consequence of this hypothesis, we can assign in the volume dV a concentration profile $d(t, z; \boldsymbol{x}), z \in (0, \Delta l)$, depending only on z, that is the axial coordinate along the normal direction $\boldsymbol{a}_3$.

This is a common basis to develop different multiscale models described in the following sections.

3.1 A preliminary model: the Higuchi formula

In order to build up a model for drug release from stents, a possible approach is to apply the principles of the Higuchi model, (proposed in [10]) into a multiscale framework. When the initial charge of the drug in the polymeric substrate is comparable with solubility of the drug, the Higuchi model is analogous to the heat conduction problem through a *semi-indefinite* and planar slab, where the heat is initially homogeneously dispersed and where the external medium acts as a perfect sink. Under these simplified conditions, it is possible to derive an explicit formula for the concentration $d(t, z; \boldsymbol{x})$ where $z \in (-\infty, 0)$, see [1] and [4]. Precisely, we obtain the similarity solutions,

$$\frac{d(t, z; \boldsymbol{x})}{d_s} = 1 - \operatorname{erf}\left(\frac{z}{\sqrt{4 D_c t}}\right), \ z \in (-\infty, 0), \ t \in (0, T], \ \boldsymbol{x} \in \Gamma,$$

where d_s is the solubility of the drug, assumed to be equivalent to the initial concentration inside the coating, namely $d_s = d_0$. Owing to the Fick's law of diffusion, from the previous expression we calculate the flux of drug J that is released per unit surface at time t,

$$J(t; \boldsymbol{x}) = -D_c \partial_z d(t, z = 0; \boldsymbol{x}) = \sqrt{\frac{D_c d_s^2}{\pi t}}, \ t \in (0, T], \ \boldsymbol{x} \in \Gamma. \tag{7}$$

We observe that $J(t;\boldsymbol{x})$ does not depend on $\boldsymbol{x} \in \Gamma$, consequently we simply write $J(t)$. This expression can be exploited to replace the governing equation of the drug concentration into the stent coating, namely $(2)_b$, by means of a Neumann-type boundary condition providing the drug release rate into the arterial walls. This condition complements the equations governing a and b. Precisely, by virtue of the Higuchi formula, problem (2) becomes,

$$\begin{cases} \partial_t a + \mathfrak{L}_w a + \mathfrak{N}_w(a,b) = 0, & \text{in } (0,T] \times \Omega_w, \\ \partial_t b + \mathfrak{N}_w(a,b) = 0, & \text{in } (0,T] \times \Omega_w, \\ \mathfrak{B}_w a = 0, & \text{on } (0,T] \times \partial\Omega_w \setminus \Gamma, \\ \mathfrak{B}_{hig}\ a = 0, & \text{on } (0,T] \times \Gamma, \end{cases} \tag{8}$$

where $\mathfrak{B}_{hig}\ a := D_w \nabla a \cdot \boldsymbol{n}_w - J(t)$.

This model gives a very simple law for the release dynamics, without solving any differential problem into the stent coating. We notice that expression (7) represents exactly the release dynamics in the limit $t \to 0$, but it is inaccurate for long time scales when the finite thickness of the coating influence the release process. Indeed, denoting with $q(t)$ the amount of drug released at time t, and with $q(\infty)$ the total amount of drug charged in the coating at the initial time, owing to (7) we obtain that the *fraction* of drug that has been released at time t is given by,

$$f(t) := \frac{q(t)}{q(\infty)} = \sqrt{\frac{4D_c t}{\pi \Delta l^2}}, \tag{9}$$

where Δl represents the uniform thickness of the stent coating. We observe that the quantity $f(t)$ reaches the value 1 in a finite time. In other words, for the Higuchi model the total amount of drug that is released is unbounded on any arbitrarily long period. This limitation is mainly due to the simplifying assumptions of the model, which do not allow to account for the equilibrium of the concentration gradients between the polymer matrix and the arterial walls. In the following section we aim to override these drawbacks.

3.2 An improved model for long time scales

We apply the analogy of the diffusion problem inside the stent coating with the *unsteady-state* heat conduction in a uniform slab of *finite thickness* equal to Δl. A similar approach has already been applied in [21] to describe the interaction between Ω_c and Ω_w in a simplified 1D setting. However, in the present work, we apply some analytical tools similar to the ones proposed in [21] with the aim to develop a multiscale model in a general 3D setting.

To start with, we propose the following approximate model for the dy-

namics of the drug inside the coating,

$$\begin{cases} \partial_t \widetilde{d} - D_c\, \partial_z^2 \widetilde{d} = 0 & \text{in } (0,T] \times (0, \Delta l), \\ \partial_z \widetilde{d} = 0 & \text{on } (0,T] \times \{z = 0\}, \\ \widetilde{d} = \alpha & \text{on } (0,T] \times \{z = \Delta l\}, \\ \widetilde{d} = d_0 & \text{on } \{t = 0\} \times (0, \Delta l), \end{cases} \tag{10}$$

where α is a constant parameter which represents the drug concentration of the external medium. This problem admits the following similarity solutions,

$$\frac{\widetilde{d}(t,z) - \alpha}{d_0 - \alpha} = s(t,z) := \sum_{n=0}^{\infty} \frac{2(-1)^n}{(n+1/2)\pi} e^{-(n+1/2)^2 kt} \cos\Big(\Big(n + \frac{1}{2}\Big)\pi \frac{z}{\Delta l}\Big), \tag{11}$$

where $k = \pi^2 D_c / \Delta l^2$, see [1].

Then, we remind that the transmission conditions imply that $d(t, z = \Delta l; \boldsymbol{x}) = a(t, \boldsymbol{x})$ for any $\boldsymbol{x} \in \Gamma$. Furthermore, we observe that the analysis of the problem, see in particular Propositions 3 and 4, allows us to conclude that $a(t, \boldsymbol{x})$ is a positive function and it is monotonically increasing with respect to t for a suitably small period. Finally, we notice that $a(t, \boldsymbol{x})$ satisfy the additional assumption to be *quasi-steady*. More precisely, since $|\Omega_w| \gg |\Omega_c|$, the time evolution of $a(t, \boldsymbol{x})$, $\boldsymbol{x} \in \Gamma$, is much slower than the variation of the concentration $d(t, z; \boldsymbol{x})$ inside the coating.

In this setting, we identify the parameter α of model (10) with the function $a(t, \boldsymbol{x})$ and we assume that the adimensional concentration inside the coating is given by expression (11). However, the scaling factor now depends on the variable concentration $a(t, \boldsymbol{x})$ instead of the constant parameter α. Precisely, we have,

$$\frac{d(t, z; \boldsymbol{x}) - a(t, \boldsymbol{x})}{d_0 - a(t, \boldsymbol{x})} = s(t, z). \tag{12}$$

It is clear that the function $d(t, z; \boldsymbol{x})$ does not satisfies problem (2) exactly, but it is a good approximation of the solution owing to the particular behavior of $a(t, \boldsymbol{x})$.

In order to couple the coating with the arterial wall we exploit the transmission condition that requires the continuity of the fluxes. By means of the Fick's law of diffusion and thanks to (12), we have

$$J(t, \boldsymbol{x}) = -D_c \partial_z d(t, \Delta l; \boldsymbol{x}) = \varphi_1(t)(d_0 - a(t, \boldsymbol{x})), \tag{13}$$

where $J(t, \boldsymbol{x})$ is the flux of drug (per unit of surface) outgoing Γ and entering Ω_w and we have set

$$\varphi_1(t) := \frac{2D_c}{\Delta l} \psi(t), \quad \psi(t) := \sum_{n=0}^{\infty} e^{-(n+1/2)^2 kt}.$$

Moreover, let $\rho(t,\boldsymbol{x})$ be the mean value of the drug concentration in the volume dV, precisely,

$$\rho(t,\boldsymbol{x}) := \frac{1}{dV}\int_{dV} d(t,z;\boldsymbol{x})\,d\omega = \frac{1}{\Delta l d\sigma}\int_0^{\Delta l} d(t,z;\boldsymbol{x})\,dz \\ = \big(\varphi_2(t)d_0 + \varphi_3(t)a(t,\boldsymbol{x})\big), \quad (14)$$

where

$$\varphi_2(t) := 2\phi(t), \quad \varphi_3(t) := 1 - 2\phi(t), \quad \phi(t) = \sum_{n=0}^{\infty} \frac{e^{-(n+1/2)^2 kt}}{(n+1/2)^2\pi^2}.$$

In conclusion, replacing equation $(2)_b$ with a boundary condition arising from the simplified model given by equation (12), problem (2) reduces to the following,

$$\begin{cases} \partial_t a + \mathfrak{L}_w a + \mathfrak{N}_w(a,b) = 0, & \text{in } (0,T]\times\Omega_w, \\ \partial_t b + \mathfrak{N}_w(a,b) = 0, & \text{in } (0,T]\times\Omega_w, \\ \mathfrak{B}_w a = 0, & \text{on } (0,T]\times\partial\Omega_w\setminus\Gamma, \\ \mathfrak{B} a = 0, & \text{on } (0,T]\times\Gamma. \end{cases} \quad (15)$$

where, owing to (13) we obtain that

$$\mathfrak{B}a := D_w\nabla a\cdot\boldsymbol{n}_w + \varphi_1(t)(a-d_0), \quad \text{on } \Gamma, \quad (16)$$

and the dynamics of the drug inside the coating is described by (14).

We notice that the transmission conditions $\mathfrak{B}(a,d) = 0$ are now replaced by $\mathfrak{B}a = 0$ on Γ, that is a simple Robin-type boundary condition complementing the first equation of (15). Although this model is formally similar to (8), it has the advantage to account for a possible growth of $a(t,\boldsymbol{x})$ and of the fact that the thickness of the coating is finite and rather small. By consequence, we expect that the present model will be more suitable than the Higuchi's one for the study of drug release over long time scales. Conversely, both models (15) and (8) are accurate for the initial phase of the release process.

Remark 3.1 We finally observe that the previous analysis can be extended putting together equation (13) and (14) by means of the mass conservation principle. The application of this principle in the control volume dV gives,

$$dV\partial_t\rho(t,\boldsymbol{x}) = -d\sigma J(t,\boldsymbol{x}),$$

and substituting (13) and (14), we obtain

$$2d_t\varphi_2(t)\big(d_0 - a(t,\boldsymbol{x})\big) + \varphi_3(t)\partial_t a(t,\boldsymbol{x}) = \frac{2D_c\psi(t)}{\Delta l^2}\big(a(t,\boldsymbol{x}) - d_0\big),$$

leading to an ordinary differential equation for each point $\boldsymbol{x} \in \Gamma$, which completely determines the evolution in time of $a(t, \boldsymbol{x})$ for $\boldsymbol{x} \in \Gamma$. Then, the Robin boundary condition (16) can be equivalently replaced by a Dirichlet-type condition providing the value of $a(t, \boldsymbol{x})$ on $(0, T] \times \Gamma$. This observation allows us to set up a multiscale model analogous to (15) in the case where the stent is covered by a topcoat to slow down the release process, see remark 2.1.

4 Numerical discretization

In a general three dimensional setting, it is not possible to further simplify problem (15). In order to obtain an approximate solution, we need to resort to suitable numerical discretization techniques.

4.1 The time advancing scheme

We notice that the Higuchi formula (7) immediately suggests that the rate of change of the concentrations in the coating and the arterial walls is extremely high at the beginning of the process and very slow at the end of it. Consequently, the set up of an effective adaptive strategy for the time step Δt^n is a crucial requirement to accurately capture the dynamics of the drug release. We present here the time discretization scheme in a general framework, and we will address the definition of the adaptive strategy later on.

Let us introduce a partition of the global time interval into subintervals whose length is non-uniform. Given $t^0 = 0$, let us set $t^n = t^{n-1} + \Delta t^n$, $n \in \mathbb{N}$, for a suitable time step $\Delta t^n > 0$. Then, given a function ξ depending on t we set $\xi^n = \xi(t^n)$. Therefore, using an implicit Euler scheme, the time discretization of the reduced model given by (14)-(15) at time t^n, reads as follows,

$$\begin{cases} \dfrac{a^n - a^{n-1}}{\Delta t^n} + \mathfrak{L}_w a^n + \mathfrak{R}_w(a^n, b^n) = 0, & \text{in } \Omega_w, \\ \dfrac{b^n - b^{n-1}}{\Delta t^n} + \mathfrak{R}_w(a^n, b^n) = 0, & \text{in } \Omega_w, \\ \mathfrak{B}_w a^n = 0, & \text{on } \partial\Omega_w \setminus \Gamma, \\ \mathfrak{B}^n a^n := D_w \nabla a^n \cdot \boldsymbol{n}_w + \varphi_1^n (a^n - d_0) = 0, & \text{on } \Gamma, \end{cases} \tag{17}$$

$$\rho^n = \left(\varphi_2^n d_0 + \varphi_3^n a^n\right), \text{ on } \Gamma. \tag{18}$$

Finally, we observe that the dynamics of drug release are effectively described by the evolution of the amount of drug in the stent $M_c(t)$ and in the

wall $M_w(t)$. At each time step t^n these quantities are given by,

$$M_w^n = \int_{\Omega_w} \left(a^n(\boldsymbol{x}) + c^n(\boldsymbol{x})\right) dV, \quad M_c^n = \Delta l \int_\Gamma \rho^n(\boldsymbol{x}) d\sigma. \tag{19}$$

4.2 Finite element approximation

Let us introduce the following inner products

$$(\boldsymbol{w}, \boldsymbol{v})_{\Omega_w} = \int_{\Omega_w} \boldsymbol{w} \cdot \boldsymbol{v}\, d\omega, \qquad (\boldsymbol{w}, \boldsymbol{v})_\Sigma = \int_\Sigma \boldsymbol{w} \cdot \boldsymbol{v}\, d\sigma,$$

where $\Sigma \subset \partial\Omega_w$. Moreover, we consider the space $\boldsymbol{W} = \{\boldsymbol{w} \in \boldsymbol{L}^2(\Omega_w) : \nabla \cdot \boldsymbol{w} \in L^2(\Omega_w),\ \boldsymbol{w} \cdot \boldsymbol{n}_w = 0\ \forall \boldsymbol{x} \in \Gamma_w \cup \Gamma\}$, where L^2 is the usual Lebesgue space and we denote with bold face the spaces of vector functions.

Let us start by considering the weak formulation related to the Darcy problem (3). Let us introduce the following bilinear form:

$$c(q, \boldsymbol{v}) = -\int_{\Omega_w} q \nabla \cdot \boldsymbol{v}\, d\omega,$$

Then, the variational formulation related to system (3) reads as follows.

Problem 1 *Find $\bar{\boldsymbol{u}} \in \boldsymbol{W}$ and $\bar{p} \in L^2(\Omega_w)$ such that,*

$$\begin{aligned} &\frac{k_b}{\mu_b}(\bar{\boldsymbol{u}}, \boldsymbol{v})_\Omega + c(\bar{p}, \boldsymbol{v}) = -\int_{\Gamma_i} \boldsymbol{v} \cdot \boldsymbol{n}_w, && \forall \boldsymbol{v} \in \boldsymbol{W}, \\ &c(q, \bar{\boldsymbol{u}}) = 0, && \forall q \in L^2(\Omega_w). \end{aligned}$$

To proceed, we assume that Ω_w can be approximated by means of a polyhedron. Then, let T_h be an admissible and quasi-uniform triangulation of Ω_w. Furthermore, we assume that the interface Γ can be approximated by means of the faces of T_h.

For the discretization of problem 1 we consider a mixed-hybrid finite element formulation based on Raviart-Thomas elements, for which we refer to [2]. By means of this method we approximate $\left[\bar{\boldsymbol{u}}, \bar{p}\right]$ by means of $\left[\tilde{\boldsymbol{u}}_h, \tilde{p}_h\right]_K \in \left[\mathbb{RT}^0, \mathbb{P}^0\right]$ for any element $K \in T_h$. Then, the velocity $\tilde{\boldsymbol{u}}_h$ is projected by means of the standard L^2 inner product on the space $\boldsymbol{X}_h^1$ of vector valued linear finite elements on T_h. By this way, we obtain $\bar{\boldsymbol{u}}_h$. Finally, for each t^n, the value of $\boldsymbol{u}_h^n \in \boldsymbol{X}_h^1$ is computed according to equation $(3)_b$.

Now, let us detail the space discretization of system (17). We notice that the weak solution a^n of problem (17) should be sought in the Sobolev space $H^1(\Omega_w)$, while ρ^n belongs to $H^{1/2}(\Gamma)$, the space of the traces on Γ of functions belonging to $H^1(\Omega_w)$, see [7]. The solution b^n of (17) also belongs to $H^1(\Omega_w)$, provided that the coefficients of the problem are regular.

Then, let $V_h := X_h^1$ be the space of the piecewise linear and continuous finite elements on T_h. This is the space where we set up the discrete weak counterpart of (17). Correspondingly, being Λ_h the space of piecewise linear and continuous functions on the faces of T_h that belong to Γ, we have $\rho_h \in \Lambda_h$. Finally, let $N_h := \dim(V_h)$ and $M_h := \dim(\Lambda_h)$ be the number of degrees of freedom of our discrete problem.

Given $\boldsymbol{u}_h^n$, the numerical approximation at time t^n of (3), let us introduce the bilinear forms associated to the second order operator $\mathfrak{L}_w$ and to the nonlinear term $\mathfrak{N}_w$, complemented by the boundary conditions given by $\mathfrak{B}_w$ and $\mathfrak{B}^n$. More precisely, $\forall a_h,\, v_h \in V_h$, we set

$$\begin{aligned}\mathcal{L}_w^n(a_h, v_h) :=& D_w(\nabla a_h, \nabla v_h)_{\Omega_w} + (\boldsymbol{u}_h^n \cdot \nabla a_h, v_h)_{\Omega_w} + \varphi_1^n(a_h, v_h)_\Gamma + P_w(a_h, v_h)_{\Gamma_i},\\ \mathcal{G}_{\mathcal{L}}^n(v_h) :=& \varphi_1^n(d_0, v_h)_\Gamma,\end{aligned}$$

that are the discrete weak counterpart of $\mathfrak{L}_w a,\ \mathfrak{B}_w a,\ \mathfrak{B}_w^n a$, while the following forms,

$$\begin{aligned}&\mathcal{N}_w(a_h, b_h, v_h) := k_1(a_h b_h, v_h)_{\Omega_w} + k_2(b_h, v_h)_{\Omega_w},\ \forall a_h,\, b_h,\, v_h \in V_h,\\ &\mathcal{G}_{\mathcal{N}}(v_h) := k_2(b_0, v_h)_{\Omega_w},\ \forall v_h \in V_h,\end{aligned}$$

correspond to the nonlinear term $\mathfrak{N}_w(a_h, b_h)$. Then, the discrete weak formulation of problem (17) reads as follows.

Problem 2 *Given $\boldsymbol{u}_h^n$, the numerical solution of (3) at time t^n, and given $a_h^{n-1}, b_h^{n-1} \in V_h$ and $\rho_h^{n-1} \in \Lambda_h$, find a_h^n and $b_h^n \in V_h$ such that for all $v_h \in V_h$,*

$$\begin{cases} \frac{1}{\Delta t^n}(a_h^n - a_h^{n-1}, v_h)_{\Omega_w} + \mathcal{L}_w^n(a_h^n, v_h) + \mathcal{N}_w(a_h^n, b_h^n, v_h) = \mathcal{G}_{\mathcal{L}}^n(v_h) + \mathcal{G}_{\mathcal{N}}(v_h), \\ \frac{1}{\Delta t^n}(b_h^n - b_h^{n-1}, v_h)_{\Omega_w} + \mathcal{N}_w(a_h^n, b_h^n, v_h) = \mathcal{G}_{\mathcal{N}}(v_h). \end{cases} \tag{20}$$

Then compute $\rho_h^n \in \Lambda_h$ given by (18).

Problem 2 can be further split into a sequence of linear problems by means of an iterative method that will be addressed in detail in Algorithm 1. Then, the convergence with respect to h and Δt of each linearized subproblem can be analyzed in the framework of numerical approximation of linear parabolic problems. We refer for instance to [23], and in particular to Corollary 11.3.1, Ch. 11, for a convergence result that exactly fits our case. Clearly, we expect first order convergence with respect to both Δt and h. This can be regarded as a considerable limitation of the present study. Moreover, we observe that our discretization scheme is not conservative with respect to the space discretization. By consequence, the mass conservation principle is not locally respected. A possibility, to improve this situation is to consider a Runge-Kutta/Discontinuous-Galerkin (RK/DG) scheme, see

[3] for the case of convection-diffusion equations. Such scheme looks particularly effective to our case because it merges the conservativity of the DG discretization with the high accuracy of the RK schemes to advance in time. Furthermore, it is also particularly suited to treat non-linear problems. The efficacy of such scheme will be addressed in a forthcoming study.

Let us now introduce the algebraic counterpart of Problem 2. To this aim, we introduce ξ_k, $k = 1, \dots, N_h$, the standard Lagrangian basis functions of V_h. Moreover, let $\boldsymbol{a}$, $\boldsymbol{b}$, $\boldsymbol{c} \in \mathbb{R}^{N_h}$ and $\boldsymbol{\rho} \in \mathbb{R}^{M_h}$ the vectors that correspond to the expansion of a_h, b_h, c_h and ρ_h with respect to the basis ξ_k. We remind that c_h is given by $c_h = b_0 - b_h$. For such vectors we introduce the following discrete norms,

$$\|\boldsymbol{v}\|_w := \|v_h\|_{L^1(\Omega_w)} \quad \text{and} \quad \|\boldsymbol{v}\|_\Gamma := \|v_h\|_{L^1(\Gamma)}.$$

If a_h^n and c_h^n are positive functions, owing to (19) we notice that $\|\boldsymbol{a}\|_w + \|\boldsymbol{c}\|_w$ corresponds to the total amount of drug present in the arterial wall. This property will be useful later on. In this setting, the bilinear form $\mathcal{L}_w$ corresponds to the following matrix,

$$\begin{aligned}\big[\mathrm{L}_w^n\big]_{ij} &:= \mathcal{L}_w^n(\xi_j, \xi_i) \\ &= D_w(\nabla\xi_j, \nabla\xi_i)_{\Omega_w} + (\boldsymbol{u}_h^n \cdot \nabla\xi_j, \xi_i)_{\Omega_w} + \varphi_1^n(\xi_j, \xi_i)_\Gamma + P_w(\xi_j, \xi_i)_{\Gamma_i}.\end{aligned}$$

In order to set up the algebraic counterpart of $\mathcal{N}_w(a_h^n, b_h^n, \xi_i)$ we introduce the following matrices,

$$\big[\mathrm{N}_w(\boldsymbol{b})\big]_{ij} := k_1 \int_{\Omega_w} \sum_{k=1}^{N_h} [\boldsymbol{b}]_k \xi_k \xi_i \xi_j, \;\; \big[\mathrm{N}_w(\boldsymbol{a})\big]_{ij} := k_1 \int_{\Omega_w} \sum_{k=1}^{N_h} [\boldsymbol{a}]_k \xi_k \xi_i \xi_j. \quad (21)$$

Moreover, we denote with

$$\big[M\big]_{ij} = (\xi_j, \xi_i)_{\Omega_w}, \qquad \big[M^\Gamma\big]_{ij} = (\xi_j, \xi_i)_\Gamma, \qquad i, j = 1, \dots, N_h,$$

the mass matrices related to the domain Ω_w and to the interface Γ respectively. According to this notation, the algebraic problem related to problem (20) reads as follows.

Problem 3 *Given $\boldsymbol{u}_h^n$, $\boldsymbol{a}^{n-1} \in \mathbb{R}^{N_h}$, $\boldsymbol{b}^{n-1} \in \mathbb{R}^{N_h}$ and $\boldsymbol{\rho}^{n-1} \in \mathbb{R}^{M_h}$, find $\boldsymbol{a}^n$ and $\boldsymbol{b}^n \in \mathbb{R}^{N_h}$ such that*

$$\begin{cases} \big(\frac{1}{\Delta t^n} M + L_w^n + N_w(\boldsymbol{b}^n)\big)\boldsymbol{a}^n + k_2 M \boldsymbol{b}^n = \boldsymbol{g}_L^n, \\ \big(\frac{1}{\Delta t^n} M + N_w(\boldsymbol{a}^n) + k_2 M\big)\boldsymbol{b}^n = \boldsymbol{g}_N^n, \end{cases} \quad (22)$$

where the right hand sides $\boldsymbol{g}_L^n, \boldsymbol{g}_N^n$ correspond to the following expressions,

$$\begin{aligned}\boldsymbol{g}_L^n &= \frac{1}{\Delta t^n} M \boldsymbol{a}^{n-1} + \varphi_1^n M^\Gamma \boldsymbol{d}^0 + k_2 M \boldsymbol{b}^0, \\ \boldsymbol{g}_N^n &= \frac{1}{\Delta t^n} M \boldsymbol{b}^{n-1} + k_2 M \boldsymbol{b}^0.\end{aligned}$$

Then, compute $\boldsymbol{\rho}^n \in \mathbb{R}^{M_h}$ *with*

$$\boldsymbol{\rho}^n = \varphi_2^n \boldsymbol{d}^0 + \varphi_3^n \boldsymbol{a}^n \qquad on\ \Gamma. \tag{23}$$

To proceed, we observe that Problem 3 is a system of two coupled and nonlinear algebraic equations in the unknowns $\boldsymbol{a}^n$ and $\boldsymbol{b}^n$, whose solution requires to resort to an iterative method. In particular, omitting for the sake of clearness the temporal index n, we consider the following fixed-point iterations.

Algorithm 1 *For any* $n > 0$*, given an admissible initial guess, for instance* $\boldsymbol{a}^{(0)} = \boldsymbol{a}^{n-1}$, $\boldsymbol{b}^{(0)} = \boldsymbol{b}^{n-1}$*, for* $k = 1, 2, \ldots$ *find a sequence* $\boldsymbol{a}^{(k)}$, $\boldsymbol{b}^{(k)}$ *such that*

$$\begin{cases} \big(\frac{1}{\Delta t} M + L_w\big)\boldsymbol{a}^{(k)} + N_w(\boldsymbol{b}^{(k-1)})\boldsymbol{a}^{(k-1)} + k_2 M \boldsymbol{b}^{(k-1)} = \boldsymbol{g}_L, \\ \big(\frac{1}{\Delta t} M + k_2 M\big)\boldsymbol{b}^{(k)} + N_w(\boldsymbol{a}^{(k-1)})\boldsymbol{b}^{(k-1)} = \boldsymbol{g}_N. \end{cases}$$

The iterations are arrested when the following convergence test is satisfied for a suitable tolerance,

$$\frac{\|\boldsymbol{a}^{(k)} - \boldsymbol{a}^{(k-1)}\|_w}{\|\boldsymbol{a}^{(k)}\|_w} + \frac{\|\boldsymbol{b}^{(k)} - \boldsymbol{b}^{(k-1)}\|_w}{\|\boldsymbol{b}^{(k)}\|_w} < tol.$$

The convergence of Algorithm 1 is stated by the following result.

Lemma 3 *For any* $n > 0$*, if* Δt^n *is small enough, the nonlinear system of equations* (22) *in Problem 3 admits an unique solution that is the limit of the sequence defined by algorithm 1 for any choice of the initial guess.*

Proof. Let us rewrite system (22) as a fixed point problem (omitting for the sake of simplicity the index n), precisely $\boldsymbol{F}(\boldsymbol{z}) = \boldsymbol{z}$, where

$$\boldsymbol{z} = \begin{bmatrix} \boldsymbol{a} \\ \boldsymbol{b} \end{bmatrix} \text{ and } \boldsymbol{F} = \begin{bmatrix} \Delta t(M + \Delta t L_w)^{-1}\big(\boldsymbol{g}_L - k_2 M \boldsymbol{b} - N_w(\boldsymbol{b})\boldsymbol{a}\big) \\ \Delta t(M + \Delta t k_2 M)^{-1}\big(\boldsymbol{g}_N - N_w(\boldsymbol{a})\boldsymbol{b}\big) \end{bmatrix}.$$

Owing to (21), we observe that for any closed subset $D \in \mathbb{R}^{N_h}$ and for any $\boldsymbol{p}$, $\boldsymbol{q}$, $\boldsymbol{r}$, $\boldsymbol{s} \in D$, the following inequality holds true,

$$\|N_w(\boldsymbol{p})\boldsymbol{q} - N_w(\boldsymbol{r})\boldsymbol{s}\| \leq \max_{\boldsymbol{p},\boldsymbol{r} \in D} \big[\|N_w(\boldsymbol{p})\|, \|N_w(\boldsymbol{r})\|\big] \|\boldsymbol{q} - \boldsymbol{s}\|. \tag{24}$$

For simplicity we denote $C := \max_{\boldsymbol{p},\boldsymbol{r} \in D} \big[\|N_w(\boldsymbol{p})\|, \|N_w(\boldsymbol{r})\|\big]$. Then, for any two points $\boldsymbol{z} = [\boldsymbol{p}, \boldsymbol{q}]^T$ and $\boldsymbol{y} = [\boldsymbol{r}, \boldsymbol{s}]^T \in \mathbb{R}^{N_h} \times \mathbb{R}^{N_h}$ endowed with the

Euclidean norm $\|\boldsymbol{z}\|^2 = \|\boldsymbol{p}\|^2 + \|\boldsymbol{q}\|^2$, exploiting (24) we obtain,

$$\|\boldsymbol{F}(\boldsymbol{z}) - \boldsymbol{F}(\boldsymbol{y})\|^2 =$$

$$\begin{aligned}
=&\| - \Delta t\, k_2\, (M + \Delta t L_w)^{-1} M(\boldsymbol{q} - \boldsymbol{s}) - \Delta t\, (M + \Delta t L_w)^{-1}\, (N_w(\boldsymbol{q})\boldsymbol{p} - N_w(\boldsymbol{s})\boldsymbol{r})\|^2 \\
&+ \| - \Delta t\, (M + \Delta t k_2 M)^{-1}\, (N_w(\boldsymbol{p})\boldsymbol{q} - N_w(\boldsymbol{r})\boldsymbol{s})\|^2
\end{aligned}$$

$$\begin{aligned}
\leq&\Delta t^2\, k_2^2\, \|(M + \Delta t L_w)^{-1} M\|^2\, \|\boldsymbol{q} - \boldsymbol{s}\|^2 + \Delta t^2\, \|(M + \Delta t L_w)^{-1}\|^2\, C^2\, \|\boldsymbol{p} - \boldsymbol{r}\|^2 \\
&+ C^2 \left(\frac{\Delta t}{1 + \Delta t k_2}\right)^2 \|M^{-1}\|^2\, \|\boldsymbol{q} - \boldsymbol{s}\|^2.
\end{aligned}$$

By observing that $\lim_{\Delta t \to 0}(M + \Delta t L_w)^{-1} = M^{-1}$, we can state that $\boldsymbol{F}$ is a contraction if Δt is small enough. Then, the result follows from standard application of the contraction mapping theorem (see, e.g., [16]). □

We point out that in Algorithm 1 we treat the non-linear term explicitly, since it makes easier to pursue the convergence analysis. However, in the numerical experiments we consider a semi-implicit treatment of the non-linear terms, because the latter scheme is expected to converge slightly faster than the former one.

4.3 An adaptive time stepping algorithm

We have already noticed that the drug release process features a very fast initial phase that progressively slows down approaching to an equilibrium state. From the mathematical point of view, this means that the simulation of the drug release requires the application of an adaptive stepping strategy to maintain a reasonable computational cost.

Although the Higuchi formula is an approximate model for long time scales, by virtue of its simplicity it turns out to be extremely useful to set up or to suitably tune an adaptive time stepping strategy. Since we are mainly interested in the analysis of the release process, we set up an adaptivity strategy based on the *increment* of the amount of drug that is released from the stent to the arterial walls. In other words, we aim to find a suitable sequence of time steps, t^n, such that a constant fraction of the total amount of drug is released in each time slab. We notice that this problem can be solved exactly in the framework of the Higuchi model.

First of all, expression (9) allows us to estimate when most of the drug will be released into the arterial walls. In particular, setting $f(t) = 1$ into (9) we obtain that the *emptying time* of the stent coating is given by,

$$t_e := \frac{\pi \Delta l^2}{4 D_c}.$$

Proceeding similarly, we compute a sequence of time steps that satisfy our objective. By definition, we know that the image of the time integration

interval $[0, t_e]$ through the function $f(t)$ is the unit interval $[0, 1]$. Then, let η be the constant fraction of drug that we aim to release at each time step. Let us introduce a uniform partition of $[0, 1]$ into sub-intervals of length η, such that $N := 1/\eta$ is an integer, for simplicity. Correspondingly, we define the sequence $f^n = n\eta$ with $n = 0, \ldots, N$. The time steps that we look for correspond to the mapping of the sequence f^n into the interval $[0, t_e]$ by means of equation (9). Precisely, we obtain,

$$t^n = \frac{\pi \Delta l^2}{4 D_c} (f^n)^2, \quad n = 0, \ldots, N, \tag{25}$$

$$\Delta t^n = \frac{\pi \Delta l^2}{4 D_c} \big[(f^n)^2 - (f^{n-1})^2 \big] = \frac{\pi \Delta l^2}{4 D_c} \eta^2 (2n - 1), \quad n = 1, \ldots, N. \tag{26}$$

This is an *a-priori* adaptive strategy for the time steps. We notice that the sequence Δt^n grows linearly. According to the restrictions of the Higuchi model, this strategy should be particularly effective at the beginning of the release process, but it is not completely reliable for long time scales.

To override this drawback, we aim to extend the ideas underlying (25) and (26) to a more general framework. We adopt the strategy proposed in [14] to set up an adaptive time stepping algorithm based on the increment. In particular, reminding that $c(t, \boldsymbol{x}) = b_0 - b(t, \boldsymbol{x})$ represents the concentration of the drug attached to the extra-cellular matrix, we address the quantity,

$$\eta^n := \frac{\|\boldsymbol{a}^n - \boldsymbol{a}^{n-1}\|_w + \|\boldsymbol{c}^n - \boldsymbol{c}^{n-1}\|_w + \Delta l \|\boldsymbol{\rho}^n - \boldsymbol{\rho}^{n-1}\|_\Gamma}{\|\boldsymbol{a}^n\|_w + \|\boldsymbol{c}^n\|_w + \Delta l \|\boldsymbol{\rho}^n\|_\Gamma} \ .$$

Owing to the definition of $\|\cdot\|_w$ and $\|\cdot\|_\Gamma$, it corresponds to the increment of the total amount of drug that is released from the stent coating plus the amount that enters the arterial walls within each time step. By virtue of the mass conservation principle, these quantities should be equivalent in a closed system. By consequence, we conclude that $\eta^n \simeq 2\eta$, where η appears into (26). Then, starting from the time step Δt^n suggested by (26), we aim to suitably correct it when it is not optimal. In particular, we notice that (26) provides a recipe to compute Δt^n given Δt^{n-1}, more precisely,

$$\mu_1^n := \frac{\Delta t^n}{\Delta t^{n-1}} = \frac{2n-1}{2n-3}, \ n = 2, \ldots, N.$$

Then, in order to maintain η^n to be bounded into a suitable interval, namely $\eta_{min} \leq \eta^n \leq \eta_{max}$, the time step Δt^n is modified according to constant de-refinement and refinement correction factors, $\mu_2 > 1, \sigma_2 = 1/\mu_2$ respectively. In particular, we choose the interval (η_{min}, η_{max}) such that $\frac{1}{2}(\eta_{min} + \eta_{max}) \simeq 2\eta$, according to the heuristic criterion $\eta^n \simeq 2\eta$. Furthermore, the de-refinement parameter is chosen such that $\mu_2 = (\eta_{min} + \eta_{max})/(2\eta_{min})$, in order to make sure that the time step is suitably rescaled when η^n goes slightly out of the bounds (η_{min}, η_{max}). We observe that all these settings

finally depend on the reference increment η. The corresponding adaptive scheme is translated in the following algorithm.

Algorithm 2 *Given* Δt_{min}, Δt_{max}, $\boldsymbol{a}^{n-1}$, $\boldsymbol{c}^{n-1}$, $\boldsymbol{\rho}^{n-1}$ *and* $\Delta\widetilde{t}^n = \mu_1^n\ \Delta t^{n-1}$, *we carry out the following steps:*

Solve. *By means of Algorithm 1, find* $\widetilde{\boldsymbol{a}}^n$, $\widetilde{\boldsymbol{c}}^n$, $\widetilde{\boldsymbol{\rho}}^n$ *the solution of Problem 3 and compute the increment,*

$$\widetilde{\eta}^n := \frac{\|\widetilde{\boldsymbol{a}}^n - \boldsymbol{a}^{n-1}\|_w + \|\widetilde{\boldsymbol{c}}^n - \boldsymbol{c}^{n-1}\|_w + \Delta l\|\widetilde{\boldsymbol{\rho}}^n - \boldsymbol{\rho}^{n-1}\|_\Gamma}{\|\widetilde{\boldsymbol{a}}^n\|_w + \|\widetilde{\boldsymbol{c}}^n\|_w + \Delta l\|\widetilde{\boldsymbol{\rho}}^n\|_\Gamma}\ .$$

Test. *According to* $\widetilde{\eta}^n$, *three options are available:*

If $\widetilde{\eta}^n > \eta_{max}$ **refine and iterate:** *set* $\Delta\widetilde{t}^n = max\{\sigma_2\Delta\widetilde{t}^n, \Delta t_{min}\}$ *and go back to* **solve.**

If $\widetilde{\eta}^n < \eta_{min}$ **de-refine and advance:** *set* $\Delta t^n = min\{\mu_2\Delta\widetilde{t}^n, \Delta t_{max}\}$, $\boldsymbol{a}^n = \widetilde{\boldsymbol{a}}^n$, $\boldsymbol{c}^n = \widetilde{\boldsymbol{c}}^n$, $\boldsymbol{\rho}^n = \widetilde{\boldsymbol{\rho}}^n$ *and go to the following time step.*

If $\eta_{min} \leq \widetilde{\eta}^n \leq \eta_{max}$ **advance:** *set* $\Delta t^n = \Delta\widetilde{t}^n$, $\boldsymbol{a}^n = \widetilde{\boldsymbol{a}}^n$, $\boldsymbol{c}^n = \widetilde{\boldsymbol{c}}^n$, $\boldsymbol{\rho}^n = \widetilde{\boldsymbol{\rho}}^n$ *and go to the following time step.*

Reminding that our time discretization scheme is only first order accurate, the key point is to choose a suitably small increment, η, that ensures an effective compromise between computational efforts and accuracy, in particular mass conservation. In alternative, more advanced schemes can be addressed, based for instance on the estimation of the local truncation error rather than the increment, see for instance [8].

5 Numerical results

In this section, we present some numerical results in order to assess the efficacy of the multiscale model proposed in Sect. 3. In particular, we consider the computational domain in Fig. 2, left, representing a portion of a truncated coronary vessel, whose radius is $1.3\,mm$, in which a drug eluting stent is implanted, as depicted in Figure 2, right. The virtual thickness of the stent is given by $\Delta l = 7 \cdot 10^{-3}\,mm$. To create this deformed domain, a finite element simulation of the expansion of the vessel has been performed in order to approximate the displacement of the arterial wall under the force due to the growth of the ballon on which the stent is placed. This study is reported in [19].

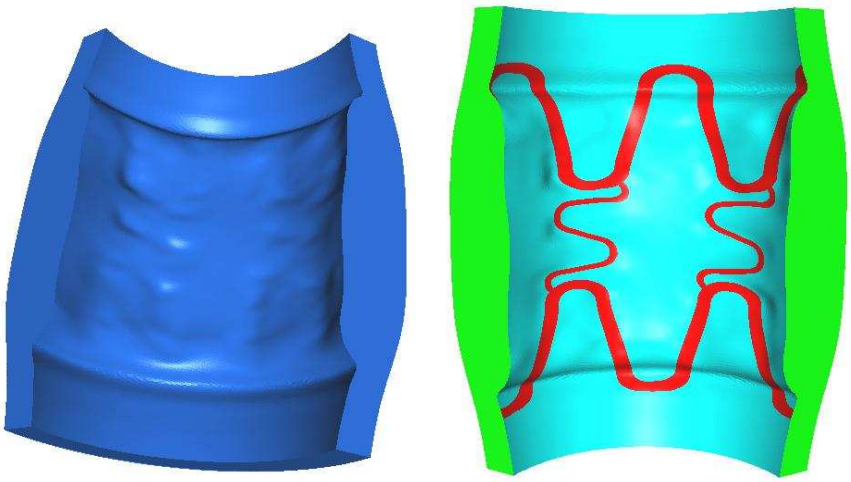

Figure 2: Computational domain (left) and a detail of the interface Γ (red color, right).

Then, an appropriate tetrahedral finite element grid has been generated using the mesh generator GAMBIT (Gambit, Fluent Inc., Labanon, NH, USA). Local grid refinement near the interface to the stent strut is applied to capture the expected high concentration gradients, for a total number of 1098680 elements. Both the Darcy Problem 1 and the mass transfer Problem 2 are solved with the finite element library *LIFE V*, written in *C++* and developed at MOX - Politecnico di Milano, INRIA - Paris and CMCS - EPFL - Lausanne, see `www.lifev.org`.

Finally, to perform the numerical simulations we use the following values for the parameters that correspond to the release of heparin and are necessary to set up problem (2): $D_w = 7.7{\cdot}10^{-6}\, mm^2/s$, $D_c = 5{\cdot}10^{-10}\, mm^2/s$, $P_w = 2 \cdot 10^{-7}\, mm/s$, $b_0 = 0.5$, $k_1 = 1\, mm^3/(mol\, s)$, $k_2 = 10^{-2}$. We refer to [26] for the values of k_1, k_2 and to [19, 17] for a discussion of the remaining ones. With these parameters we obtain $t_e \simeq 1$ day. In this case, accounting for the pulsatile pressure variations into the Darcy model turns out to be a very demanding task from the computational point of view. By consequence, we do not include this feature in our simulations and we set $\delta p = 70\, mmHg$.

As regards the set up of the time step adaptivity strategy, we consider $\eta = 2 \cdot 10^{-3}$ into (26) and thus $N = 500$. According to the heuristic criterion $\eta^n \simeq 2\eta$ we choose $\eta_{min} = 3 \cdot 10^{-3}$ and $\eta_{max} = 5 \cdot 10^{-3}$ such that $\frac{1}{2}(\eta_{min} + \eta_{max}) = 2\eta$. Then, we obtain the value of the de-refinement factor of Algorithm 2 from the expression $\mu_2 := (\eta_{min} + \eta_{max})/(2\eta_{min}) = 1.333$. Moreover we set $\Delta t_{min} = 0.1$s and $\Delta t_{max} = 600$s$= 10$min. In figure 3 we compare the sequences Δt^n and $\Delta \widetilde{t}^n$ generated by equation (26) and Algorithm 2 respectively. We notice that they satisfy $\Delta t^n \leq \Delta \widetilde{t}^n$ for any $n > 0$

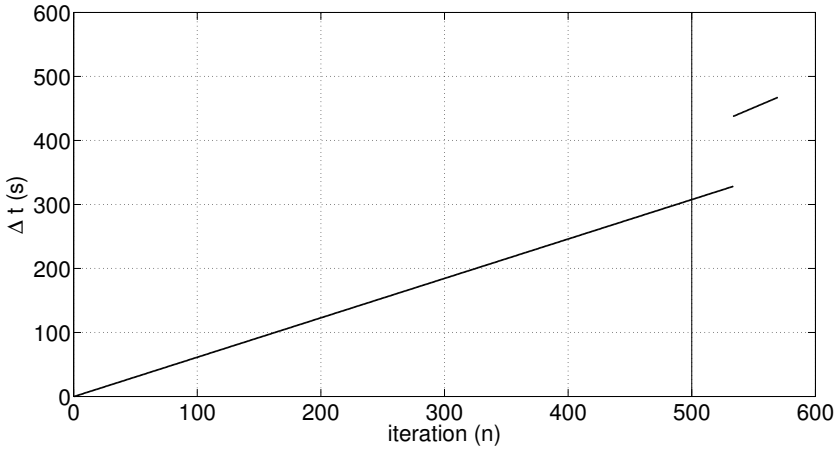

Figure 3: Adaptive time step Δt.

and in particular $\Delta t^n = \Delta \widetilde{t}^n$ for $0 < n \leq N = 500$ that is the range where equations (25) and (26) can be applied. Consequently, only the step *advance* occurs along the execution of Algorithm 2, that is $\eta_{min} \leq \widetilde{\eta}^n \leq \eta_{max}$. This confirms that the a-priori adaptivity strategy based on the Higuchi model turns out to be effective also in the case of model (15).

Concerning the physiological interpretation of the results, we show in Fig. 4 the concentration of the free drug and of the corresponding free binding sites at different times. We notice that the drug is progressively transferred from the stent to the neighboring arterial wall, and even after a relatively long time, e.g. 1 day, the distribution of the drug inside the wall is substantially influenced by the geometrical design of the stent.

In Fig. 5 we show the dynamics of $M_c(t)$ and $M_w(t)$ for model (15). Their values are normalized with respect to the total amount of drug. First of all, we notice that almost the 50% of the drug is lost by diffusion into the blood flow through the interface between the lumen and the arterial wall. Secondly, we observe that the concentration of the drug in the vessel wall is mainly present in the state c rather than the state a. This is explained observing that the direct reaction (1) is much faster than the inverse one because in our case $k_1 >> k_2$. Indeed, most of the drug is permanently attached to the specific sites of the extra-cellular matrix of the tissue. From the applicative point of view, this fact has both favorable and adverse implications. On one side it increases the residence time of the drug into the arterial walls, on the other side it prevents the uniform distribution of the drug.

Finally, in figure Fig. 6 we compare the release profiles $M_c(t)$ and $M_w(t)$ of models (8) and (15). We observe that model (15) can be applied to study the drug release on an arbitrarily long time scale that can exceed the emptying time t_e, highlighted with a vertical line. Furthermore, comparing the

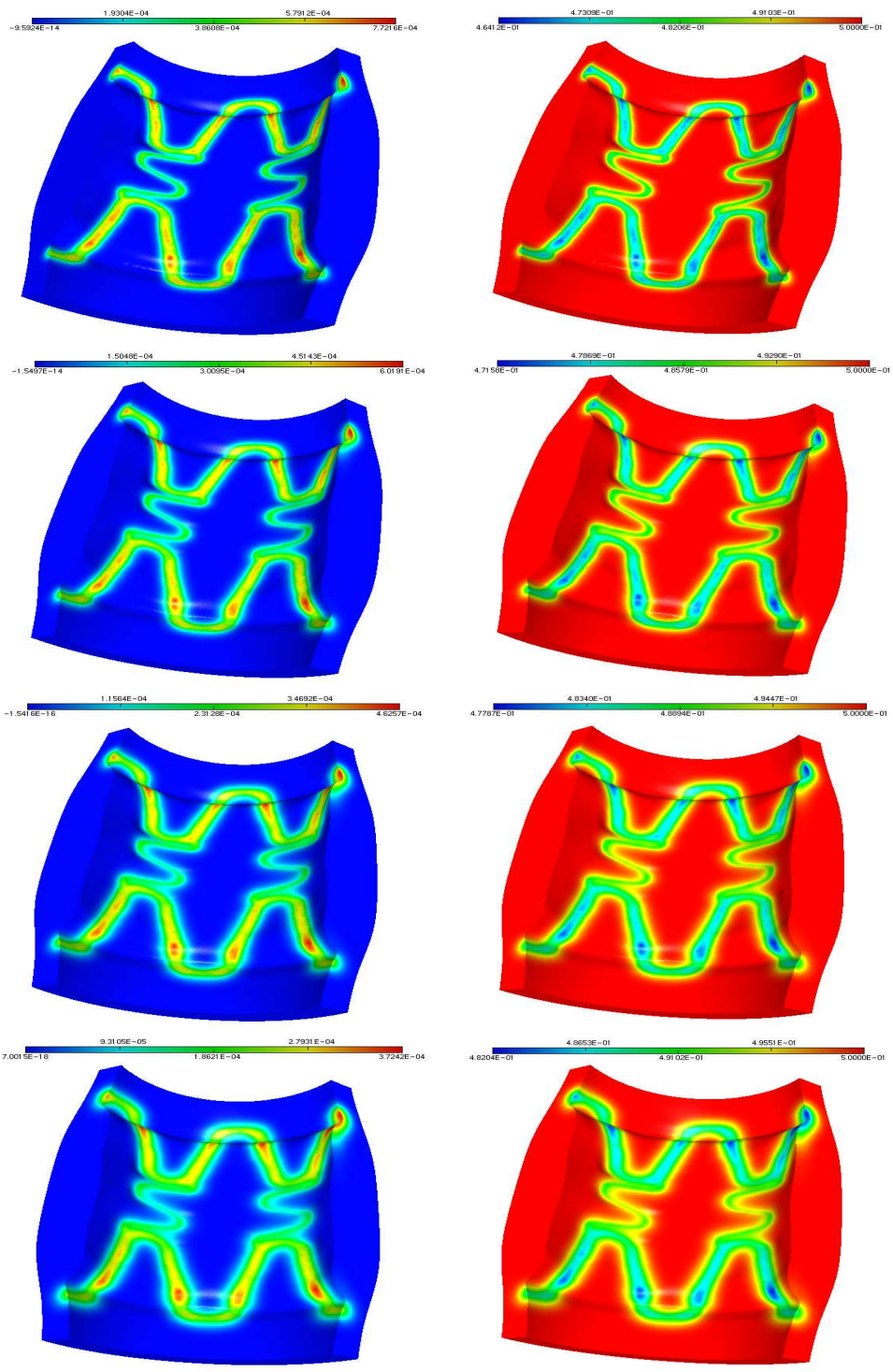

Figure 4: The concentration of the dissolved drug after 6, 12, 18 and 24 hours is reported on the left from top to bottom. On the right, the corresponding concentration of the free binding sites is depicted.

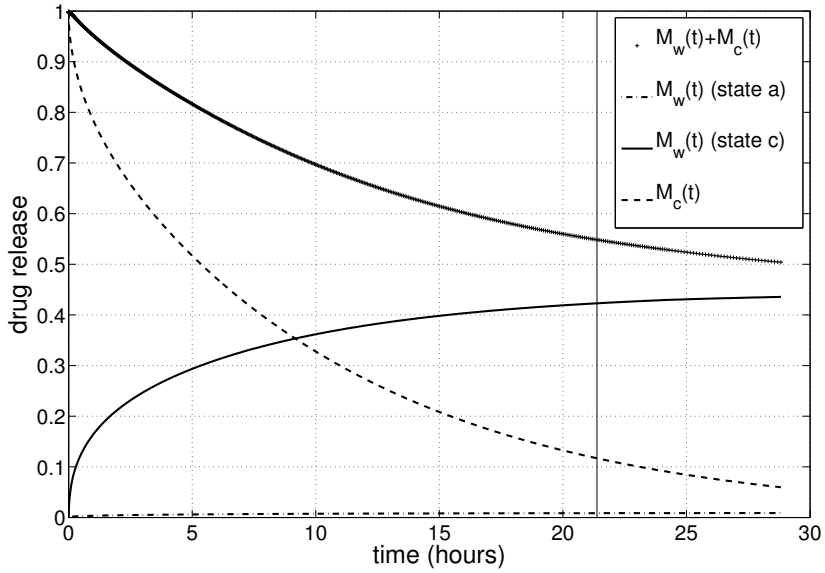

Figure 5: The dynamics of $M_c(t)$ and $M_w(t)$ for model (15).

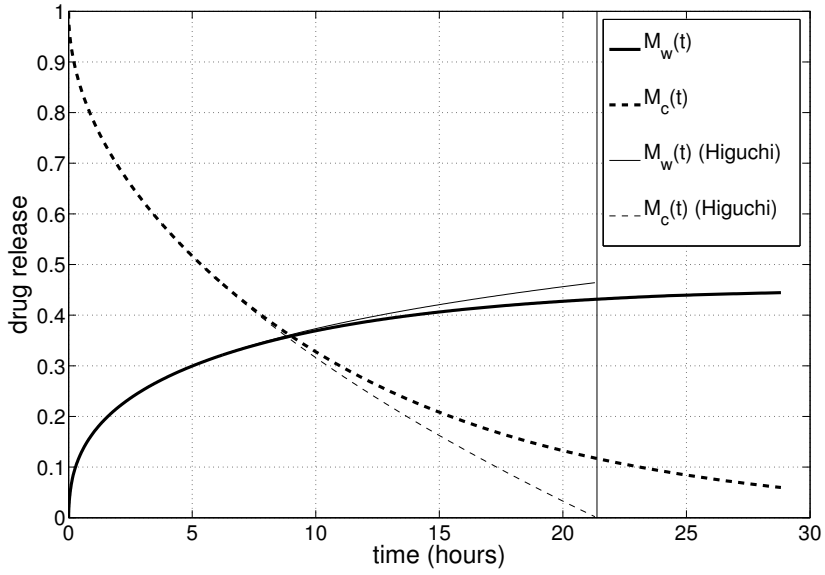

Figure 6: A comparison of models (8) and (15).

release profiles for models (8) and (15), we observe that the latter provides a release rate slower than the Higuchi model, especially for long time scales, when the concentration gradients between the stent and the arterial walls become negligible. These observations agree with the more realistic basic assumptions at the basis of model (15).

6 Concluding remarks

The multiscale method and the corresponding numerical scheme illustrated in this work represent a novel and effective technique to describe the drug release from a cardiovascular stent. This approach makes it possible to satisfy the main requirements of the application at hand, which consist on accounting for the very complex geometrical design involving different space scales and on following the dynamics of the system for a long time period. Finally, this methodology is not restricted to stents, but could also be useful for any application where a drug or other chemical substances are slowly released from a thin layer coating a device.

Acknowledgments

This work has been supported by Fondazione Cariplo, Milan, Italy, under the project "Modellistica matematica di materiali microstrutturati per dispositivi a rilascio di farmaco", by the Italian Institute of Technology (Istituto Italiano di Tecnologie) with the project "NanoBiotechnology - Models and Methods for Local Drug Delivery from Nano/Micro Structured Materials" and by the Policlinico di Milano with the project "Sistemi di Bioingegneria virtuale: Realizzazione di un modello per la identificazione e correzione dei difetti nel Sistema Venoso". The authors gratefully acknowledge F. Gervaso, F. Migliavacca and G. Dubini at LaBS, Dipartimento di Strutturale, Politecnico di Milano, who have provided the computational domain and have given many suggestions, and M. Prosi and S. Minisini for the support in *LifeV*.

References

[1] R.B. Bird, W.E. Stewart, and E.N. Lightfoot. *Transport Phenomena*. John Wiley, 1966.

[2] G. Chavent and J.E. Roberts. A unified physical presentation of mixed, mixed-hybrid finite elements and standard finite-difference approximations for the determination of velocities in waterflow problems. *Advances in Water Resources*, 14(6):329–348, 1991.

[3] Bernardo Cockburn and Chi-Wang Shu. The local discontinuous Galerkin method for time-dependent convection-diffusion systems. *SIAM J. Numer. Anal.*, 35(6):2440–2463 (electronic), 1998.

[4] Donald S. Cohen and Thomas Erneux. Controlled drug release asymptotics. *SIAM J. Appl. Math.*, 58(4):1193–1204 (electronic), 1998.

[5] Michel C. Delfour, André Garon, and Vito Longo. Modeling and design of coated stents to optimize the effect of the dose. *SIAM J. Appl. Math.*, 65(3):858–881 (electronic), 2005.

[6] D. Fry. Mathematical models of arterial transmural transport. *Am. J. Physiol.*, 248(2):H240–H263, 1985.

[7] David Gilbarg and Neil S. Trudinger. *Elliptic partial differential equations of second order*. Classics in Mathematics. Springer-Verlag, Berlin, 2001. Reprint of the 1998 edition.

[8] E. Hairer and G. Wanner. *Solving ordinary differential equations. II*, volume 14 of *Springer Series in Computational Mathematics*. Springer-Verlag, Berlin, second edition, 1996. Stiff and differential-algebraic problems.

[9] Philip Hartman. *Ordinary differential equations*, volume 38 of *Classics in Applied Mathematics*. Society for Industrial and Applied Mathematics (SIAM), Philadelphia, PA, 2002. Corrected reprint of the second (1982) edition [Birkhäuser, Boston, MA; MR0658490 (83e:34002)], With a foreword by Peter Bates.

[10] T. Higuchi. Rate of release of medicaments from ointment bases containing drugs in suspension. *J. Pharmac. Sci.*, 50:874–875, 1961.

[11] T. Higuchi. Mechanism of sustained-action medication - theoretical analysis of rate of release of solid drugs dispersed in solid matrices. *J. Pharmac. Sci.*, 52:1145–1149, 1963.

[12] D.R. Hose, A.J. Narracott, B. Griffiths, S. Mahmood, J. Gunn, D. Sweeney, and P.V. Lawford. A thermal analogy for modelling drug elution from cardiovascular stents. *Computer Methods in Biomechanics and Biomedical Engineering*, 7:257–264, 2004.

[13] C. Hwang, D. Wu, and E.R. Edelman. Physiological transport forces govern drugdistribution for stent-based delivery. *Circulation*, 104(5):600–605, 2001.

[14] Alessandra Jannelli and Riccardo Fazio. Adaptive stiff solvers at low accuracy and complexity. *J. Comput. Appl. Math.*, 191(2):246–258, 2006.

[15] G. Karner and K. Perktold. Effect of endothelial injury and increased blood pressure on albumin accumulation in the arterial wall: a numerical study. *J. Biomech.*, 33:709–715, 2000.

[16] C. T. Kelley. *Iterative methods for linear and nonlinear equations*, volume 16 of *Frontiers in Applied Mathematics*. Society for Industrial and Applied Mathematics (SIAM), Philadelphia, PA, 1995. With separately available software.

[17] M.A. Lovich and E.R. Edelman. Ecomputational simulations of local vascular heparin deposition and distribution. *Am. J. Physiol.*, 271:214–224, 1996.

[18] Panos Macheras and Athanassios Iliadis. *Modeling in biopharmaceutics, pharmacokinetics, and pharmacodynamics*, volume 30 of *Interdisciplinary Applied Mathematics*. Springer, New York, 2006. Homogeneous and heterogeneous approaches.

[19] F. Migliavacca, F. Gervaso, M. Prosi, P. Zunino, S. Minisini, L. Formaggia, and G. Dubini. Expansion and drug elution model of a coronary stent. *Computer Methods in Biomechanics and Biomedical Engineering*, 10:63–73, 2007.

[20] C. V. Pao. *Nonlinear parabolic and elliptic equations*. Plenum Press, New York, 1992.

[21] G. Pontrelli and de Monte F. Mass diffusion through two-layer porous media: an application to the drug-eluting stent. *International Journal of Heat and Mass Transfer*, 50:3658–3669, 2007.

[22] M. Prosi, P. Zunino, K. Perktold, and A. Quarteroni. Mathematical and numerical models for transfer of low-density lipoproteins through the arterial walls: a new methodology for the model set up with applications to the study of disturbed lumenal flow. *J. Biomech.*, 38:903–917, 2005.

[23] Alfio Quarteroni and Alberto Valli. *Numerical approximation of partial differential equations*, volume 23 of *Springer Series in Computational Mathematics*. Springer-Verlag, Berlin, 1994.

[24] Alfio Quarteroni and Alberto Valli. *Domain decomposition methods for partial differential equations*. Numerical Mathematics and Scientific Computation. The Clarendon Press Oxford University Press, New York, 1999. , Oxford Science Publications.

[25] Alfio Quarteroni, Alessandro Veneziani, and Paolo Zunino. Mathematical and numerical modeling of solute dynamics in blood flow and arterial walls. *SIAM J. Numer. Anal.*, 39(5):1488–1511 (electronic), 2001/02.

[26] D.V. Sakharov, L.V. Kalachev, and D.C. Rijken. Numerical simulation of local pharmacokinetics of a drug after intravascular delivery with an eluting stent. *J. Drug Targ.*, 10(6):507–513, 2002.

MOX Technical Reports, last issues

Dipartimento di Matematica "F. Brioschi",
Politecnico di Milano, Via Bonardi 9 - 20133 Milano (Italy)

15/2007 C. Vergara, P. Zunino:
Multiscale modeling and simulation of drug release from cardiovascular stents

14/2007 L. Dedé:
Reduced Basis Method for Parametrized Advection-Reaction Problems

13/2007 P. Zunino:
Discontinuous Galerkin methods based on weighted interior penalties for second order PDEs with non-smooth coefficients

12/2007 A. Deponti, L. Bonaventura, G. Rosatti, G. Garegnani:
An Accurate and Efficient Semi-Implicit Method for Section Averaged Free Surface Flow Modelling

11/2007 S. Badia, F. Nobile, C. Vergara:
Fluid-structure partitioned procedures based on Robin transmission conditions

10/2007 N. Parolini, A. Quarteroni:
Modelling and Numerical Simulation for Yacht Engineering

09/2007 C. May, N. Flournoy:
Asymptotics in response-adaptive designs generated by a two-colors, randomly reinforced urn

08/2007 L. Formaggia, E. Miglio, A. Mola, N. Parolini:
Fluid-structure interaction problems in free surface flows: application to boat dynamics

07/2007 A. Ern, A. E. Stephansen, P. Zunino:
A Discontinuous Galerkin method with weighted averages for advection-diffusion equations with locally vanishing and anisotropic diffusivity

06/2007 A. Deponti, L. Bonaventura, L. Fraccarollo, E. Miglio, G. Rosatti:
Analysis of Hyperbolic Systems for Mobile–Bed, Free–Surface Flow Modelling in Arbitrary Cross Sections